Chemical Science

ROYAL SOCIETY OF CHEMISTRY

EDGE ARTICLE

View Article Online
View Journal | View Issue

Cite this: *Chem. Sci.*, 2020, **11**, 8846

All publication charges for this article have been paid for by the Royal Society of Chemistry

Received 23rd May 2020
Accepted 15th July 2020

DOI: 10.1039/d0sc02907f

rsc.li/chemical-science

The noncovalent dimerization of a G-quadruplex/hemin DNAzyme improves its biocatalytic properties†

Yu Cheng,‡[ab] Mingpan Cheng,‡[a] Jingya Hao,[ab] Guoqing Jia,[a] David Monchaud[c] and Can Li*[a]

While many protein enzymes exert their functions through multimerization, which improves both selectivity and activity, this has not yet been demonstrated for other naturally occurring catalysts. Here, we report a multimerization effect applied to catalytic DNAs (or DNAzymes) and demonstrate that the enzymatic efficiency of G-quadruplexes (GQs) in interaction with the hemin cofactor is remarkably enhanced by homodimerization. The resulting non-covalent dimeric GQ–DNAzyme system provides hemin with a structurally defined active site in which both the cofactor (hemin) and the oxidant (H_2O_2) are activated. This new biocatalytic system efficiently performs peroxidase- and peroxygenase-type biotransformations of a broad range of substrates, thus providing new perspectives for biotechnological application of GQs.

Introduction

Besides its function as the repository of genetic information, DNA molecules are increasingly studied for their biocatalytic properties, often referred to as DNAzymes.[1–11] Catalytic DNA usually comprises a sequence in which a tertiary structure is encoded which, upon interaction with a metal cofactor,[12] accelerates chemical reactions.[13–21] An interesting tertiary structure is the G-quadruplex (GQ) that folds from guanine-rich sequences through the stacking of G-quartets, *i.e.*, arrays of four guanines associated *via* Hoogsteen hydrogen bonds.[22–26] A GQ exhibits enticing catalytic properties notably upon interaction with hemin (Fe(III)–protoporphyrin IX), a well-known cofactor of hemoproteins.[27,28] The stacking of hemin onto an accessible G-quartet of a GQ provides a catalytic GQ/hemin system that promotes peroxidase- and peroxygenase-type oxidation of different substrates in the presence of an excess of oxidants such as hydrogen peroxide (H_2O_2).[27,29] However, despite dozens of examples and applications reported each year,[12,13,30,31] the precise mechanism of these oxidations still remains unclear.

Hemin can interact with both accessible G-quartets of a GQ, referred to as the 3′- and 5′-end, respectively, but is more catalytically competent at the 3′-end.[29,32–35] Various catalytic intermediates have been postulated to explain this observation, but a firm demonstration is still expected.[36,37] Efforts have been invested to optimize the hemin binding site *via* the modification of the adjacent nucleobases or the surrounding loops of the 3′-end.[32,38–44] However, most if not all optimizations have been attempted with monomeric GQs.[45] We previously demonstrated that multimeric GQs (comprising several covalently linked GQ units) display better catalytic performance than the corresponding monomeric GQs.[46–48] This improvement originates from the formation of a high-activity hemin binding site located at the interface between two consecutive GQ units. In these assemblies, hemin is sandwiched in between the 3′-end of a GQ unit and the 5′-end of the other GQ unit (Fig. 1A).[46–48]

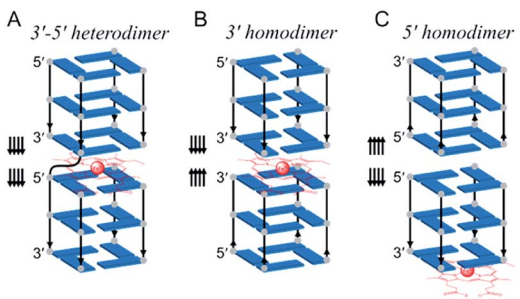

Fig. 1 Schematic representation of dimeric GQ interaction with hemin: (A) a covalent multimeric GQ considered as a 3′–5′ heterodimeric GQ;[46] two non-covalent GQ assemblies that interact *via* their 3′-ends (3′–3′ homodimeric GQ, B) and their 5′-ends (5′–5′ homodimeric GQ, C). The arrows indicate the strand orientation from the 5′- to 3′-direction; only the structural core of GQs is represented for clarity.

[a]State Key Laboratory of Catalysis, Dalian Institute of Chemical Physics, Chinese Academy of Sciences, Dalian 116023, China. E-mail: canli@dicp.ac.cn

[b]University of Chinese Academy of Sciences, Beijing 100049, China

[c]Institut de Chimie Moléculaire de l' Université de Bourgogne (ICMUB), CNRS UMR 6302, UBFC Dijon, 21078 Dijon, France

† Electronic supplementary information (ESI) available. See DOI: 10.1039/d0sc02907f

‡ These authors contributed equally.

Here, we hypothesize that providing hemin with a binding pocket formed by two 3′-ends can enhance its catalytic proficiency. To do so, we decided not to use covalent multimeric GQs (that require long sequences, *i.e.*, being poorly efficient and having expensive syntheses, and for which only 5′–3′ interfaces have been reported) but we designed 3′–3′ stacked non-covalent dimeric GQs (along with 5′–5′ dimers as controls), resulting from the self-association of two blunt-ended GQs with naked 3′-ends (and 5′-ends, respectively, Fig. 1B and C). In this original biocatalytic system, hemin nestles in between two 3′-ends (Fig. 1B) where it acquires a high catalytic activity that allows the resulting system to perform a broad variety of biotransformations in a highly efficient manner.

Results and discussion

Formation of a non-covalent dimeric GQ–DNAzyme system

An approach to control the dimerization of GQs is to use DNA sequences that fold into tetramolecular GQs (that is, with a single stretch of guanines comprising 3 to 5 guanines) with various 3′- and 5′-ends.[49–51] The 3′-homodimeric GQ system was built with 5′-TTAG$_n$-3′ (n = 3–5), displaying a blunt 3′-G-quartet, along with 5′-TTAG$_n$T-3′, 5′-TTAG$_n$TT-3′ and 5′-TTAG$_3$p-3′ (corresponding to the 5′-TTAG$_n$-3′ sequence with a 3′ phosphorylated end) as controls since the presence of dTs (or phosphate groups) on the 3′-end is likely to preclude GQ dimerization. We experimentally established this by non-denaturing polyacrylamide gel electrophoresis (PAGE) (Fig. 2A and B): in a GQ-promoting K^+-rich buffer (100 mM KCl), 5′-TTAG$_3$-3′ was predominantly found as a dimer (64% *versus* 36% as a monomer), its 3′-homodimeric nature having been previously established by nuclear magnetic resonance (NMR) spectroscopy.[52,53] Conversely, 5′-TTAG$_3$TT-3′ was found as a monomer only,[52] and both 5′-TTAG$_3$T-3′ and 5′TTAG$_3$p-3′ were found as mixtures of monomeric and dimeric forms. We confirmed this by NMR for 5′-TTAG$_3$-3′, 5′-TTAG$_3$T-3′ and 5′-TTAG$_3$TT-3′ (Fig. S1†). The 5′-homodimeric GQ system was built using 5′-(G$_3$T)$_4$-3′, 5′-T(G$_3$T)$_4$-3′ and 5′-TT(G$_3$T)$_4$-3′. These sequences were selected since it was previously demonstrated that 5′-(G$_3$T)$_4$-3′ self-assembles into a 5′-homodimer (PDB 2LE6), 5′-TT(G$_3$T)$_4$-3′ exists as a monomer only (PDB 2LK7) and 5′-T(G$_3$T)$_4$-3′ as a mixture of monomeric and dimeric forms.[54,55] To further demonstrate the generality of this approach, other sequences were studied (a total of 23 sequences, Table S1†), whose GQ folding ability was assessed by circular dichroism (CD, Fig. S2†)[56] and dimerization was assessed by PAGE (Fig. S3†).

Next, the influence of the presence of hemin was studied by both PAGE and CD (Fig. 2B and S2†): hemin was found not to disturb GQ dimerization and was even able to promote and stabilize the GQ dimer. As an example, the proportion of the dimeric form of 5′-TTAG$_3$-3′ increases from 64 to 76% (Fig. 2B) and the melting temperature (assessed by CD-melting experiment) increases by 13 °C (Fig. 2C) after the addition of hemin. This strong GQ dimer/hemin interaction thus opened the way towards the use of these new catalytic systems for performing peroxidation-like reactions. The oxidation of 2,2′-azino-bis(3-ethylbenzothiazoline-6-sulfonic acid) (ABTS) by H_2O_2 was used as a model reaction, given that it is a firmly established model reaction and it provides a readily monitorable output (appearance of a characteristic absorbance at λ = 414 nm corresponding to the product ABTS$^{\bullet+}$). To assess the performance of these new catalytic systems over a relatively long period of time (2 h), we first used a high concentration of the substrate (2 mM, Fig. 2D). We found that the relationship between homodimerization and catalytic activity was straightforward, with initial velocities (V_0) of 11 054, 5333, 1624 and 1054 nM s^{-1} for 5′-TTAG$_3$-3′, 5′-TTAG$_3$p-3′, 5′-TTAG$_3$T-3′ and 5′-TTAG$_3$TT-3′, respectively (of note is that after 10 min of reaction, the absorbance started to decrease due to the degradation of ABTS$^{\bullet+}$ under the conditions used). 5′-TTAG$_3$-3′, which is found mostly as a 3′-homodimer, is thus 11-fold more catalytically competent than 5′-TTAG$_3$TT-3′, which exists as a monomer only.

We then compared the performances of the 3′- and 5′-homodimers by decreasing the ABTS concentration (0.5 mM, Fig. 3). Only small variations in catalytic performances were monitored with the 5′-homodimers (Fig. 3A), with V_0 = 140, 172 and 142 nM s^{-1} for 5′-(G$_3$T)$_4$-3′, 5′-T(G$_3$T)$_4$-3′ and 5′-TT(G$_3$T)$_4$-3′, respectively, which are roughly 2-fold lower than that of 5′-TTAG$_3$-3′ (V_0 = 288 nM s^{-1}, Fig. 3B). The generality of this approach was demonstrated through using dAs instead of dTs

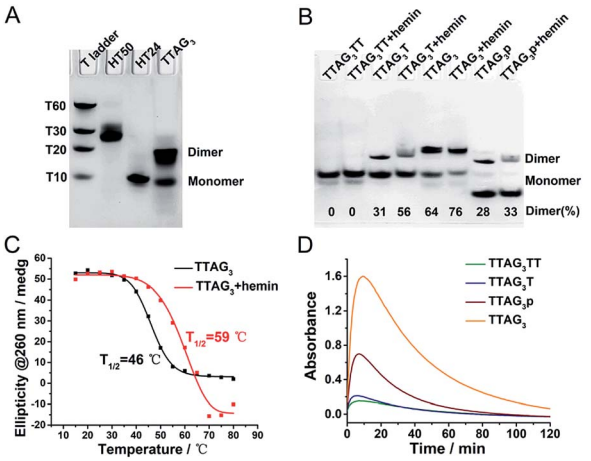

Fig. 2 (A) PAGE analysis of the dimerization of 5′-TTAG$_3$-3′ in 100 mM KCl. Oligonucleotides HT50 (5′-(TTAG$_3$)$_8$TT-3′)[57] and HT24 (5′-T$_2$-G$_3$(TTAG$_3$)$_3$A-3′, PDB# 2GKU)[58] and poly(dT)s were used as migration markers for dimeric and monomeric GQs, respectively. (B) PAGE analysis of the dimerization of 5′-TTAG$_3$TT-3′, 5′-TTAG$_3$T-3′, 5′-TTAG$_3$-3′, and 5′-TTAG$_3$p-3′ (50 μM), with and without hemin (100 μM), in 40 mM HEPES buffer (pH 7.5) with 100 mM KCl. The percentage of the dimer is given at the bottom of the gel. (C) CD-melting profiles at 260 nm of 5′-TTAG$_3$-3′ (10 μM) in the absence (black line) and presence of hemin (5 μM, red line) in 40 mM HEPES buffer (pH 7.5) with 100 mM KCl and 0.05% (v/v) Triton X-100 (Fig. S4†). (D) Catalytic oxidation of ABTS (2 mM, absorbance at λ = 414 nm as a function of the time) promoted by H_2O_2 (0.6 mM) in the presence of GQs (0.25 μM) and hemin (0.5 μM) in 40 mM HEPES buffer (pH 7.5, optimized by pH-dependent catalytic reactions, Fig. S6†) with 100 mM KCl and 0.05% (v/v) Triton X-100, at 25 °C. The initial reaction velocities (V_0) of oxidations catalyzed by 5′-TTAG$_3$TT-3′, 5′-TTAG$_3$T-3′, 5′-TTAG$_3$p-3′ and 5′-TTAG$_3$-3′ are V_0 = 11 054, 5333, 1624 and 1054 nM s^{-1}, respectively.

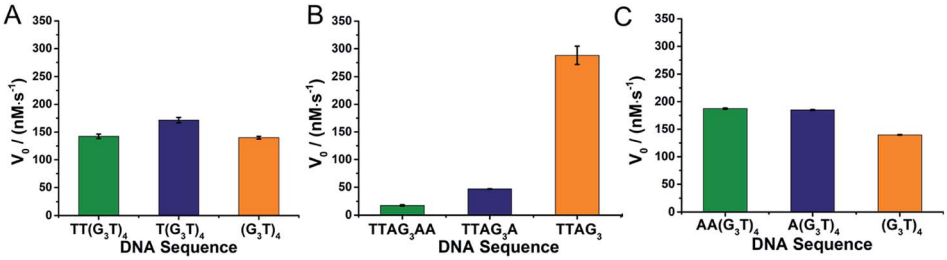

Fig. 3 Catalytic activities of non-covalent dimeric GQ–DNAzymes formed from 5′-homodimers with dTs on their 5′-ends (A, 5′-TT(G$_3$T)$_4$-3′, 5′-T(G$_3$T)$_4$-3′ and 5′-(G$_3$T)$_4$-3′), 3′-homodimers with dAs on their 3′-ends (B, 5′-TTAG$_3$AA-3′, 5′-TTAG$_3$A-3′ and 5′-TTAG$_3$-3′) and 5′-homodimers with dAs on their 5′-ends (C, 5′-AA(G$_3$T)$_4$-3′, 5′-A(G$_3$T)$_4$-3′ and 5′-(G$_3$T)$_4$-3′). The reactions were performed with GQs (0.25 μM) and hemin (0.5 μM) in the presence of ABTS (0.5 mM) and H_2O_2 (0.5 mM) in 40 mM HEPES (pH 7.5) with 100 mM KCl and 0.05% (v/v) Triton X-100, at 25 °C.

as nucleobases that disrupt GQ dimerization: again the presence of dAs had drastic consequences on the catalytic activity of the 3′-homodimers,[32,40,42] with 5′-TTAG$_3$-3′ being far more efficient than 5′-TTAG$_3$A-3′ and 5′-TTAG$_n$AA-3′ (V_0 = 288, 47 and 18 nM s^{-1}, respectively, Fig. 3B), while it barely affected those of the 5′-homodimers (V_0 = 140, 185 and 187 nM s^{-1} for 5′-(G$_3$T)$_4$-3′, 5′-A(G$_3$T)$_4$-3′ and 5′-AA(G$_3$T)$_4$-3′, respectively, Fig. 3C).

Potassium promotes GQ dimerization and DNAzyme activity

We then decided to further investigate GQ dimerization *via* ^{1}H-NMR. The analysis of 5′-TTAG$_3$-3′ was performed in the presence of increasing amounts of KCl (from 0 to 300 mM, Fig. 4A, B and S1A†). The ^{1}H-NMR signals between 10 and 12 (the so called imino protons) are characteristic of the guanines embedded in G-quartets. Our results confirmed first that the GQ was not folded without K$^+$; they also showed that monomeric GQs are favoured at low-concentration of K$^+$ and that an increase in K$^+$ concentration favoured dimeric GQs. This was further demonstrated by size exclusion chromatography (SEC)-HPLC (Fig. 4C)[59] and PAGE experiments (Fig. 4D). A comparative quantitative analysis of these two techniques showed remarkable agreement in the percentage of dimeric GQs promoted by K$^+$ (Fig. 4E), with >75% of the dimeric form in the presence of 300 mM KCl. We also verified the behaviour of both 5′-TTAG$_3$T-3′ and 5′-TTAG$_3$TT-3′ under similar conditions: as expected, the monomeric form was found to be predominant for both sequences even at 300 mM KCl concentration (Fig. S1B and C†). This K$^+$-promoted dimerization had also strong consequences in terms of biocatalysis. Indeed, varying the KCl concentration from 0 to 500 mM strongly impacted the catalytic performance of 5′-TTAG$_3$-3′ but not that of 5′-TTAG$_3$T-3′ and 5′-TTAG$_3$TT-3′: in the presence of 500 mM KCl, 5′-TTAG$_3$-3′ was found to be 41- and 10-fold more catalytically active than 5′-TTAG$_3$TT-3′ and 5′-TTAG$_3$T-3′, respectively (Fig. 4F). The straightforward relationship between the V_0 values and the percentage of dimeric GQs is unambiguously demonstrated in Fig. 4G, without being a simple linear correlation (Fig. 4H). Of note is that we demonstrated the specificity of the K$^+$ cations by replacing them with Li$^+$, Na$^+$, NH_4^+ or Mg^{2+}, which resulted in a decrease of both GQ dimerization and GQ–DNAzyme activities (Fig. S5†). We also performed these experiments at pH 7.5 and 25 °C since these conditions were found to be optimal for GQ–DNAzyme catalysis (Fig. S6†).

We finally assessed whether the 5′-TTAG$_3$-3′ dimer withstood dilution, in order to operate in the low micromolar concentration range routinely used for DNAzyme-type experiments. SEC-

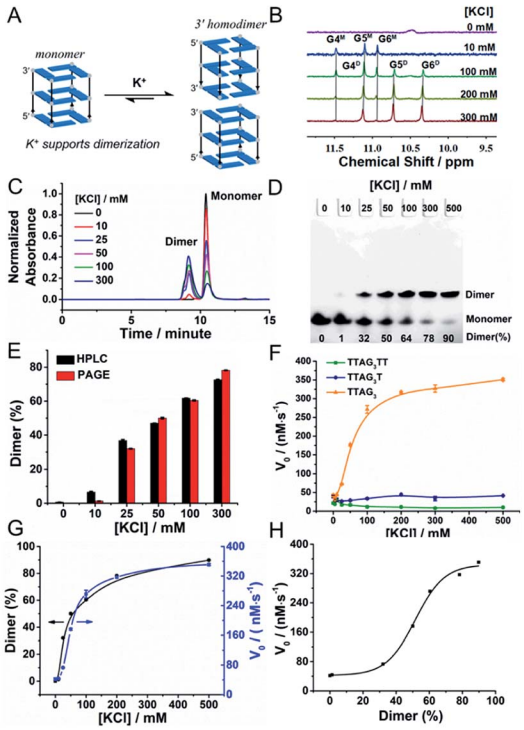

Fig. 4 Schematic representation (A) of the K$^+$-promoted GQ dimerization of 5′-TTAG$_3$-3′, ^{1}H-NMR spectra (B) of 5′-TTAG$_3$-3′ (GQ, 100 μM) at different K$^+$ concentrations (0, 10, 100, 200 and 300 mM), in 10% (v/v) D_2O/H_2O, pH/pD 7.5. The imino protons were assigned according to previously published articles;[27,42] 'M' and 'D' stand for the monomeric and dimeric GQs, respectively. Guanines are numbered according to their position in the d(T$_1$T$_2$A$_3$G$_4$G$_5$G$_6$) sequence. SEC-HPLC (C) and PAGE analysis (D) of 5′-TTAG$_3$-3′ at different K$^+$ concentrations (0 to 500 mM). (E) Comparison of the percentage of the dimeric form of 5′-TTAG$_3$-3′ obtained by both SEC-HPLC and PAGE at different K$^+$ concentrations. Catalytic activities (V_0, F) of non-covalent dimeric GQ–DNAzymes formed from 5′-TTAG$_3$-3′, 5′-TTAG$_3$T-3′ and 5′-TTAG$_3$TT-3′ as a function of the K$^+$ concentration. Comparison (G) and relationship (H) of the percentage of the dimeric GQ formed from 5′-TTAG$_3$-3′ and the catalytic activity of the 5′-TTAG$_3$-3′/hemin DNAzyme (V_0) at different K$^+$ concentrations.

HPLC and PAGE analyses showed that the percentage of the dimeric GQ did not change with dilution (Fig. S7A–C and Table S2†). The optimal concentration for GQ–DNAzyme experiments was thus determined (Fig. S7D†): the catalytic activity was found to increase rapidly with the GQ concentration in the 0–2.5 μM range and to reach a plateau after 5.0 μM. This concentration was thus chosen for subsequent studies.

Kinetics and scope of non-covalent dimeric GQ–DNAzymes

The kinetics of GQ–DNAzymes with 3′-homodimers were studied *via* the measurement of V_0 values for reactions performed with increasing H_2O_2 concentration (0 to 6 mM). The kinetic curves of 5′-TTAG$_3$-3′, 5′-TTAG$_3$T-3′, 5′-TTAG$_3$TT-3′ and 5′-TTAG$_3$p-3′ are seen in Fig. 5A and B (those of 5′-TTAG$_4$-3′, 5′-TTAG$_4$T-3′ and 5′-TTAG$_4$TT-3′ as well as 5′-TTAG$_5$-3′, 5′-TTAG$_5$T-3′ and 5′-TTAG$_5$TT-3′ in Fig. S8A†). Michaelis–Menten fitting gave the kinetic parameters k_{cat}, K_m and k_{cat}/K_m (summarized in Fig. S8B and Table S3†): the blunt-end dimeric GQs 5′-TTAG$_n$-3′ (n = 3, 4 or 5) were found to be far more efficient (k_{cat}/K_m between 1.2 and 1.6 s^{-1} mM^{-1}, Fig. 5C) than any other sequences, with k_{cat}/K_m between 4.3- and 5.4-fold higher than those of the monomeric GQs 5′-TTAG$_n$TT-3′ (n = 3, 4 or 5). The best results were obtained with 5 μM 5′-TTAG$_3$-3′ (denoted by * in Fig. 5C), with k_{cat} = 8.2 s^{-1}, K_m = 3.8 mM and k_{cat}/K_m = 2.2 s^{-1} mM^{-1}, which represent a 82-fold (k_{cat}) and 7.4-fold (k_{cat}/K_m) enhancement as compared to those of monomeric 5′-TTAG$_3$TT-3′. These results positioned the 3′-homodimeric system in the upper range of the reported k_{cat} examples (1.1, 4.2, 4.3 and 2.3 s^{-1} for PS2.M,[60] c-Myc,[60] EAD2 (ref. 60) and c-Myc3C-2A,[38] respectively), but still lower than that of horseradish peroxidase (HRP, 330 s^{-1}),[28] and in the high range of k_{cat}/K_m values (*e.g.*, 2.1 s^{-1} mM^{-1} for c-Myc3C-2A),[38] but still far lower than that of HRP (10^4 s^{-1} mM^{-1}).[28]

To further investigate the scope of applications of this new system, we studied the catalytic oxidations of eight different substrates (Fig. 6), *i.e.*, luminol,[61] TMB,[62] L-tyrosine,[63] D-tyrosine,[63] L-dopa,[63] dopamine,[63] NADH[64] and thioanisole.[29] The logic behind this selection is three-fold: first, luminol and TMB are two classical substrates for DNAzyme-based biosensors;[13] second, L/D-tyrosine, L-dopa, dopamine and NADH are naturally occurring substrates whose oxidation products are implicated in oxidative stress;[36,65,66] third, most of these substrates are an illustrative panel of organic contaminants from industrial activities. Oxidative enzymes such as HRP are indeed used for remediation purposes,[67] allowing for the treatment of wastewaters and contaminated soils, with this enzyme being effective with a wide range of substrates,[68] from organic dyes[69] to phenolic contaminants.[70] This series of dyes (luminol, ABTS and TMB), phenolic (tyrosine) and biphenolic compounds (dopamine) and a thiol derivative (thioanisole)[71] was used to assess the efficiency of both 3′-homodimers (5′-TTAG$_3$-3′, 5′-TTAG$_3$T-3′ and 5′-TTAG$_3$TT-3′) and 5′-homodimers (5′-(G$_3$T)$_4$-3′, 5′-T(G$_3$T)$_4$-3′ and 5′-TT(G$_3$T)$_4$-3′) as tools for degrading environmental pollutants. We found that the 5′-TTAG$_3$-3′ dimer strongly accelerated all these oxidations, while the dT-containing GQ and the monomeric GQs only moderately (Fig. S9†). We also checked whether some of these catalysts were asymmetric but no inductions of chirality were observed for L- and D-tyrosine (Fig. S9.3 and S9.4†), and thioanisole (see chiral HPLC traces in the ESI†), which is not unexpected given the lack of a chiral environment provided by the homodimers.

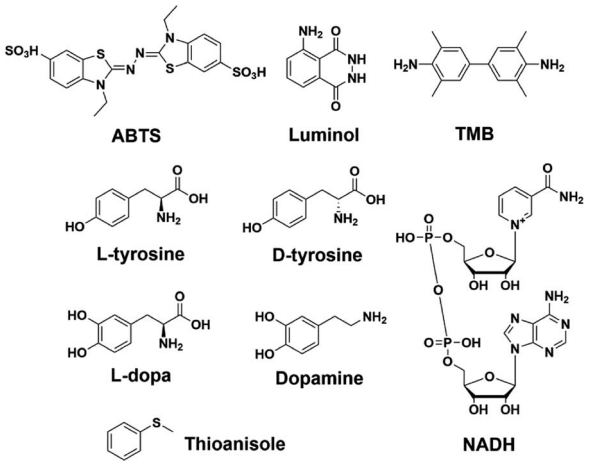

Fig. 6 Different substrates used for assessing the scope of non-covalent dimeric GQ–DNAzymes.

Model of the non-covalent dimeric GQ–DNAzyme

The actual structure of the DNAzyme system formed from the dimerization of the GQ formed using 5′-TTAG$_3$-3′, and

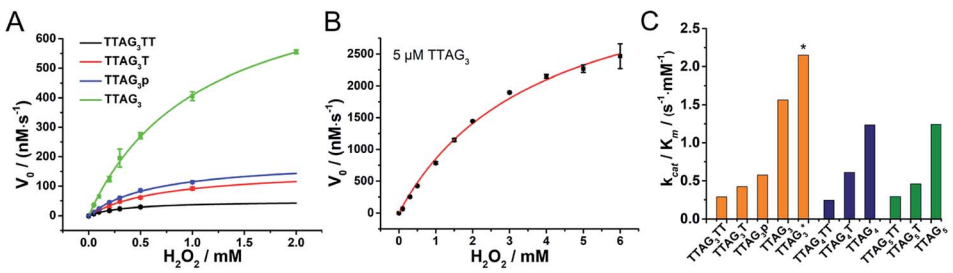

Fig. 5 Michaelis–Menten analysis of non-covalent dimeric GQ–DNAzymes from 5′-TTAG$_3$TT-3′, 5′-TTAG$_3$T-3′, 5′-TTAG$_3$p-3′ and 5′-TTAG$_3$-3′ at 0.25 μM concentration (A) and from 5′-TTAG$_3$-3′ at 5 μM concentration (B). Catalytic efficiency (k_{cat}/K_m values, C) of 3′-homodimeric DNAzymes formed from GQs (0.25 μM; * data obtained with 5 μM GQ) and hemin (0.5 μM) in the presence of ABTS (0.5 mM) at increasing H_2O_2 concentrations (0 to 6.0 mM) in 40 mM HEPES (pH 7.5) with 100 mM KCl and 0.05% (v/v), at 25 °C.

sandwiching hemin, was further investigated by SEC-HPLC. This analysis allows for both discrimination of the monomeric and dimeric GQs (absorbance of the DNA at 260 nm) and identification of the GQ/hemin complex (absorbance of hemin at 404 nm). In the absence of hemin, the results seen in Fig. 7A show that the monomeric and dimeric GQs can be easily identified; after addition of hemin, the signatures seen in Fig. 7B demonstrate both the coexistence of the monomeric and dimeric GQs (absorbance at 260 nm) in the presence of hemin (meaning that it does not affect the equilibrium, in line with the PAGE results seen in Fig. 2B) and the exclusive formation of the dimeric GQ/hemin complex (absorbance at 404 nm). These results indicated that hemin binds to the dimeric GQs only; we can thus postulate that the preferred hemin binding site is the cleft formed at the 3′–3′ interface (Fig. 1B).

To further demonstrate that the 5′-end is not involved in the catalytic properties of the resulting GQ/hemin complexes, a series of 3′-homodimers was designed with various 5′-ends (5′-TAG_3-3′, 5′-AAG_3-3′, 5′-TTG_3-3′ and 5′-ATG_3-3′). The dimerization of these sequences was checked by PAGE (Fig. S3C†). We also found that these sequences displayed similar catalytic activities (Fig. S10A†), in line with the primary role of the nature of their 3′-ends only. As controls, we disrupted the G-tract of 5′-$TTAG_3$-3′ (both 5′-TTAGCG-3′ and 5′-TTACCG-3′, Fig. S3D†); the resulting complexes did not exhibit catalytic activity (Fig. S10B†). Finally, we compared the catalytic proficiencies of the non-covalent dimer formed using 5′-$TTAG_3$-3′ and those of the covalent multimers 46AG,[46] 70AG[46] and HT50:[57] the results seen in Fig. S10C and Table S4† confirmed the far better properties, at least 22-fold higher catalytic efficiency of the non-covalent dimeric GQ precatalysts as compared to their covalently linked counterparts.

Altogether, this wealth of data lends credence to a model in which hemin becomes catalytically active once sandwiched in between the two 3′-ends of a homodimeric GQ (Fig. 1B). This hypothesis is further substantiated by recent molecular-level simulations that scrutinized GQ dimerization and highlighted the positive roles played by small-molecule ligands in the stability of the GQ/ligand/GQ assemblies at their 3′ interfaces.[51] We decided to keep on investigating the hemin/GQ interactions *via* UV-Vis titrations, and compare our results with those of known GQ–DNAzymes and enzymes (Table S5†): the evolution of the characteristic UV-Vis bands such as Soret, E and D bands (Fig. S11†) indicates that the coordination of the iron atom with the dimeric GQ is of high spin and the six-coordination (HS/6C)-type, similar to what was described with PS2.M and MetMb.[28,60] The negligible changes of these UV-Vis bands after addition of the monomeric control 5′-TAG_3TT-3′ and 5′-TAG_3-3′ at low potassium concentration demonstrated again the privileged binding of hemin to dimeric GQs (Fig. S11†). The apparent dissociation constant K_d decreased with the steric hindrance on the 3′-end (K_d = 5.96, 3.91 and 2.84 μM for 5′-$TTAG_3T$-3′, 5′-$TTAG_3$p-3′ and 5′-$TTAG_3$-3′, respectively, Table S4 and Fig. S12†), and with increasing K^+ concentrations (K_d = 5.68, 4.16, 2.84 and 0.91 μM for 5′-$TTAG_3$-3′ at 25, 50, 100 and 300 mM K^+, respectively, Table S4 and Fig. S12†), thus further accrediting the hypothesis whereby dimeric GQs provide a better binding pocket to hemin than monomeric GQs.

We next measured the formation rate of reactive intermediates (high-valent iron species) *via* the H_2O_2-mediated oxidative degradation of GQ/hemin complexes monitored *via* the time-dependent evolution of the Soret band in the absence of a reducing substrate (Fig. S14†).[66] GQ/hemin complexes formed from 10 selected sequences (Fig. 8A) were tested: the initial degradation velocities (V_d) determined indicated that complexes from the 5′-$TTAG_3$-3′ and 5′-$TTAG_4$-3′ series were degraded more quickly than the corresponding monomers, with the notable exception of the 5′-$TTAG_5$-3′ series (*vide infra*). To further illustrate this, we plotted the V_d values *versus* the k_{cat}/K_m determined above: the representation seen in Fig. 8B shows that the most catalytically competent sequences experience faster degradation. The case of 5′-$TTAG_5$-3′ is interesting since it exhibits a high catalytic activity and a low degradation rate, thereby opening new avenues towards the design of ever more competent and robust GQ–DNAzyme systems.

A mechanism of why and how GQ dimerization enhances the DNAzyme activity of the resulting complexes can be built in agreement and on the basis of previously published models[28,39,62,65,66,72,73] (Fig. 9): at the 3′–3′ interface, one of the guanines can flip out from the proximal G-quartet (a 'wobbling' guanine)[36,39,66,74] to coordinate axially to the iron atom and activate hemin while the distal G-quartet interacts with iron-bound H_2O and H_2O_2. This H-bonding contributes to the heterolysis of O–H *via* an electron-withdrawing activation. The orchestrated action of both proximal and distal G-quartets

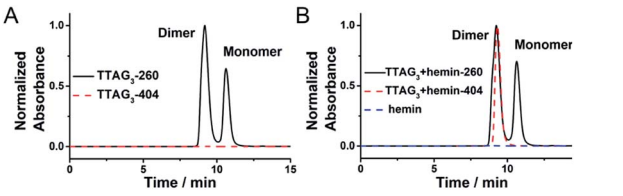

Fig. 7 SEC-HPLC profiles of 5′-$TTAG_3$-3′ (10 μM) in the absence (A) and presence (B) of hemin (2.0 μM), monitored at 260 nm (DNA absorbance, solid line) and 404 nm (hemin absorbance, dashed line) in 40 mM HEPES (pH 7.5) with 100 mM KCl.

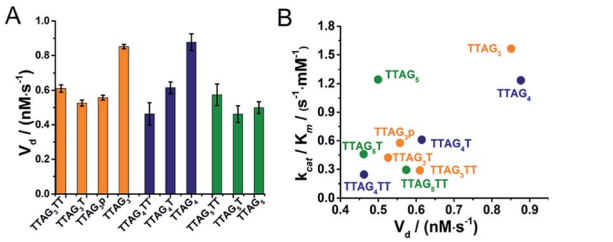

Fig. 8 Oxidative degradation of 3′-homodimeric GQ–DNAzymes monitored through the initial apparent degradation velocities (V_d, A) and the correlation between V_d and k_{cat}/K_m values (B). Reactions were performed with GQs (0.25 μM) and hemin (0.5 μM) in the presence of H_2O_2 (0.5 mM) in 40 mM HEPES (pH 7.5) with 100 mM KCl and 0.05% (v/v) Triton X-100.

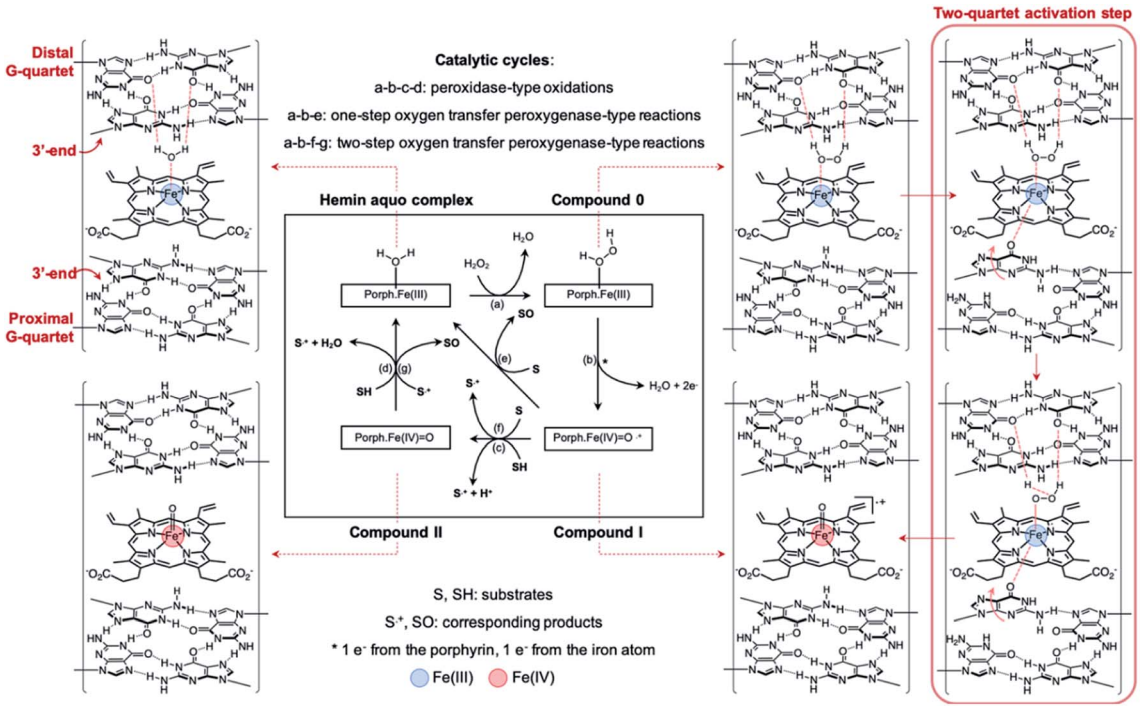

Fig. 9 Postulated mechanism in which distal and proximal G-quartets concomitantly activate both hemin and H_2O_2 to enhance the catalytic proficiency of non-covalent dimeric GQ–DNAzyme degradation systems.

uniquely provides a finely tuned hemin binding site, close to what is found in hemoproteins, which is more defined than in monomeric GQs in which one activator is the G-quartet and the other one a structurally labile adjacent nucleobase[32,38,39,42] or externally added nucleotides.[62,75,76] The presence of two G-quartets uniquely allows for a concerted mechanism (Fig. 9, right red box) that enhances the catalytic efficiency of the resulting complex *via* a concomitant activation of the cofactor and the oxidant.

Conclusion

We report here a new prototypic GQ–DNAzyme system comprising two GQ units that self-assemble in a non-covalent manner. We demonstrate that dimeric GQs provide a more defined binding pocket to hemin than monomeric GQs, in which all reaction partners (cofactor and oxidant) are concomitantly activated. The sequence used to validate this proof-of-concept derives from the human telomeric sequence 5′-TTAGGG-3′, in which the 3′-end was left naked on purpose, to make the resulting tetramolecular GQ self-assemble to form a 3′-homodimer, in light of the capacity of blunt-ended GQs to interact with each other, drawn in like magnets through hydrophobic, electrostatic and π-stacking interactions. This new system referred to as the non-covalent dimeric GQ–DNAzyme exhibits high catalytic efficiency, with k_{cat} values up to 8 s^{-1} for the ABTS oxidation. This system contributes to a new strategy to design efficient GQ–DNAzymes, which can be used to catalyse various types of biotransformations: the scope and versatility of this system were demonstrated *via* a selection of substrates that are representative of organic pollutants of anthropogenic origin. This provides interesting perspectives for the use of DNA catalysts as biosourced tools for green chemistry purposes and potential sustainable solutions to critical environmental concerns.

Conflicts of interest

There are no conflicts to declare.

Acknowledgements

We thank Dr Jean-Louis Mergny (Paris, France), Dr Jun Zhou (Nanjing University, China) and Dr Sheng-mei Lu (Dalian Institute of Chemical Physics, China) for their helpful comments on our manuscript. This work was supported by the National Major Scientific Instruments and Equipment Development Project of the National Natural Science Foundation of China, NSFC Grant (No. 2152780065), the National Key R&D Program of China (2017YFB0702800), the CNRS, the *Agence Nationale de la Recherche* (No. ANR-18-CE07-0017-03), the Université de Bourgogne and Conseil Régional de Bourgogne (PARI) and the European Union (PO FEDER-FSE Bourgogne 2014/2020 programs).

Notes and references

1 K. Kruger, P. J. Grabowski, A. J. Zaug, J. Sands, D. E. Gottschling and T. R. Cech, *Cell*, 1982, **31**, 147.

2 C. Guerrier-Takada, K. Gardiner, T. Marsh, N. Pace and S. Altman, *Cell*, 1983, **35**, 849.
3 R. R. Breaker and G. F. Joyce, *Chem. Biol.*, 1994, **1**, 223.
4 I. Willner, B. Shlyahovsky, M. Zayats and B. Willner, *Chem. Soc. Rev.*, 2008, **37**, 1153.
5 J. Liu, Z. Cao and Y. Lu, *Chem. Rev.*, 2009, **109**, 1948.
6 S. K. Silverman, *Trends Biochem. Sci.*, 2016, **41**, 595.
7 M. Liu, D. Chang and Y. Li, *Acc. Chem. Res.*, 2017, **50**, 2273.
8 D. Morrison, M. Rotherbroker and Y. Li, *Small Methods*, 2018, **2**, 1700319.
9 M. Hollenstein, *Curr. Opin. Chem. Biol.*, 2019, **52**, 93.
10 M. Cepeda-Plaza and A. Peracchi, *Org. Biomol. Chem.*, 2010, **18**, 1697.
11 L. Ma and J. Liu, *iScience*, 2020, **23**, 100815.
12 J. L. Mergny and D. Sen, *Chem. Rev.*, 2019, **119**, 6290.
13 Y. Xing, X. Liu, Q. Pu, M. Wu and J. X. Zhao, *ACS Appl. Bio Mater.*, 2018, **1**, 1019.
14 C. E. McGhee, K. Y. Loh and Y. Lu, *Curr. Opin. Biotechnol.*, 2017, **45**, 191.
15 A. Rioz-Martinez and G. Roelfes, *Chem. Biol.*, 2015, **25**, 80.
16 D. J.-F. Chinnapen and D. Sen, *Proc. Natl. Acad. Sci. U. S. A.*, 2004, **101**, 65.
17 C. Wang, G. Jia, J. Zhou, Y. Li, Y. Liu, S. Lu and C. Li, *Angew. Chem., Int. Ed.*, 2012, **51**, 9352.
18 M. Cheng, Y. Li, J. Zhou, G. Jia, S. M. Lu, Y. Yang and C. Li, *Chem. Commun.*, 2016, **52**, 9644.
19 M. Cheng, J. Hao, Y. Li, Y. Cheng, G. Jia, J. Zhou and C. Li, *Biochimie*, 2018, **146**, 20.
20 Y. Cheng, M. Cheng, J. Hao, G. Jia and C. Li, *ChemBioChem*, 2018, **19**, 2233.
21 H. Ibrahim, P. Mulyk and D. Sen, *ACS Omega*, 2019, **4**, 15280.
22 D. Rhodes and H. J. Lipps, *Nucleic Acids Res.*, 2015, **43**, 8627.
23 R. Hansel-Hertsch, M. Di Antonio and S. Balasubramanian, *Nat. Rev. Mol. Cell Biol.*, 2017, **18**, 279.
24 L. Stefan and D. Monchaud, *Nat. Rev. Chem.*, 2019, **3**, 650.
25 J. Spiegel, S. Adhikari and S. Balasubramanian, *Trends Chem.*, 2020, **2**, 123.
26 D. Varshney, J. Spiegel, K. Zyner, D. Tannahill and S. Balasubramanian, *Nat. Rev. Mol. Cell Biol.*, 2020, **21**, 459.
27 P. Travascio, Y. Li and D. Sen, *Chem. Biol.*, 1998, **5**, 505.
28 P. Travascio, A. J. Bennet, D. Y. Wang and D. Sen, *Chem. Biol.*, 1999, **6**, 779.
29 L. C. Poon, S. P. Methot, W. Morabi-Pazooki, F. Pio, A. J. Bennet and D. Sen, *J. Am. Chem. Soc.*, 2011, **133**, 1877.
30 E. Golub, R. Freeman and I. Willner, *Anal. Chem.*, 2013, **85**, 12126.
31 J. Chen, Y. Zhang, M. Cheng, J. L. Mergny, Q. Lin, J. Zhou and H. Ju, *Mikrochim. Acta*, 2019, **186**, 786.
32 W. Li, Y. Li, Z. Liu, B. Lin, H. Yi, F. Xu, Z. Nie and S. Yao, *Nucleic Acids Res.*, 2016, **44**, 7373.
33 K. Saito, H. Tai, H. Hemmi, N. Kobayashi and Y. Yamamoto, *Inorg. Chem.*, 2012, **51**, 8168.
34 T. Ai, Q. Yang, Y. Lv, Y. Huang, Y. Li, J. Geng, D. Xiao and C. Zhou, *Chem.–Asian J.*, 2018, **13**, 1805.
35 Y. Yamamoto, H. Araki, R. Shinomiya, K. Hayasaka, Y. Nakayama, K. Ochi and T. Shibata, *Biochemistry*, 2018, **57**, 5938.
36 P. Travascio, P. K. Witting, A. G. Mauk and D. Sen, *J. Am. Chem. Soc.*, 2001, **123**, 1337.
37 H. Shimizu, H. Tai, K. Saito, T. Shibata, M. Kinoshita and Y. Yamamoto, *Bull. Chem. Soc. Jpn.*, 2015, **88**, 644.
38 T. Chang, H. Gong, P. Ding, X. Liu, W. Li, T. Bing, Z. Cao and D. Shangguan, *Chem.–Eur. J.*, 2016, **22**, 4015.
39 J. Chen, Y. Zhang, M. Cheng, Y. Guo, J. Šponer, D. Monchaud, J. L. Mergny, H. Ju and J. Zhou, *ACS Catal.*, 2018, **8**, 11352.
40 Y. Guo, J. Chen, M. Cheng, D. Monchaud, J. Zhou and H. Ju, *Angew. Chem., Int. Ed.*, 2017, **56**, 16636.
41 W. Li, S. Chen, D. Xu, Q. Wen, T. Yang and J. Liu, *Chem.–Eur. J.*, 2018, **24**, 14500.
42 J. Chen, Y. Guo, J. Zhou and H. Ju, *Chem.–Eur. J.*, 2017, **23**, 4210.
43 E. Golub, H. B. Albada, W. C. Liao, Y. Biniuri and I. Willner, *J. Am. Chem. Soc.*, 2016, **138**, 164.
44 M. Cheng, J. Zhou, G. Jia, X. Ai, J. L. Mergny and C. Li, *Biochim. Biophys. Acta, Gen. Subj.*, 2017, **1861**, 1913.
45 A. Ponce-Salvatierra, K. Wawrzyniak-Turek, U. Steuerwald, C. Höbartner and V. Pena, *Nature*, 2016, **529**, 231.
46 L. Stefan, F. Denat and D. Monchaud, *J. Am. Chem. Soc.*, 2011, **133**, 20405.
47 Y. Li, G. Jia, C. Wang, M. Cheng and C. Li, *ChemBioChem*, 2015, **16**, 618.
48 Y. Li, C. Wang, J. Hao, M. Cheng, G. Jia and C. Li, *Chem. Commun.*, 2015, **51**, 13174.
49 S. Kolesnikova, M. Hubalek, L. Bednarova, J. Cvacka and E. A. Curtis, *Nucleic Acids Res.*, 2017, **45**, 8684.
50 C. J. Lech, B. Heddi and A. T. Phan, *Nucleic Acids Res.*, 2013, **41**, 2034.
51 M. Kogut, C. Kleist and J. Czub, *PLoS Comput. Biol.*, 2019, **15**, e1007383.
52 Y. Kato, T. Ohyama, H. Mita and Y. Yamamoto, *J. Am. Chem. Soc.*, 2005, **127**, 9980.
53 Y. Wang and D. J. Patel, *Biochemistry*, 1992, **31**, 8112.
54 N. Q. Do and A. T. Phan, *Chem.–Eur. J.*, 2012, **18**, 14752.
55 N. Q. Do, K. W. Lim, M. H. Teo, B. Heddi and A. T. Phan, *Nucleic Acids Res.*, 2011, **39**, 9448.
56 R. Del Villar-Guerra, J. O. Trent and J. B. Chaires, *Angew. Chem., Int. Ed.*, 2018, **57**, 7171.
57 L. Petraccone, C. Spink, J. O. Trent, N. C. Garbett, C. S. Mekmaysy, C. Giancola and J. B. Chaires, *J. Am. Chem. Soc.*, 2011, **133**, 20951.
58 K. N. Luu, A. T. Phan, V. Kuryavyi, L. Lacroix and D. J. Patel, *J. Am. Chem. Soc.*, 2006, **128**, 9963.
59 E. Largy and J. L. Mergny, *Nucleic Acids Res.*, 2014, **42**, 149.
60 X. Cheng, X. Liu, T. Bing, Z. Cao and D. Shangguan, *Biochemistry*, 2009, **48**, 7817.
61 Y. Xiao, V. Pavlov, R. Gill, T. Bourenko and I. Willner, *ChemBioChem*, 2004, **5**, 374.
62 L. Stefan, F. Denat and D. Monchaud, *Nucleic Acids Res.*, 2012, **40**, 8759–8772.
63 A. M. Rojas, P. A. Gonzalez, E. Antipov and A. M. Klibanov, *Biotechnol. Lett.*, 2007, **29**, 227.
64 E. Golub, R. Freeman and I. Willner, *Angew. Chem., Int. Ed.*, 2011, **50**, 11710.

65 D. Sen and L. C. Poon, *Crit. Rev. Biochem. Mol. Biol.*, 2011, **46**, 478.
66 J. Wang, M. Cheng, J. Chen, H. Ju, D. Monchaud, J.-L. Mergny and J. Zhou, *Chem. Commun.*, 2020, **56**, 1839.
67 N. Durán and E. Esposito, *Appl. Catal., B*, 2000, **28**, 83.
68 T. Rasheed, M. Bilal, F. Nabeel, M. Adeel and H. M. N. Iqbal, *Environ. Int.*, 2019, **122**, 52.
69 Q. Husain, *Rev. Environ. Sci. Biotechnol.*, 2009, **9**, 117.
70 G. R. Lopes, D. C. G. A. Pinto and A. M. S. Silva, *RSC Adv.*, 2014, **4**, 37244.
71 S. Zhao, H. Xi, Y. Zuo, S. Han, Y. Zhu, Z. Li, L. Yuan, Z. Wang and C. Liu, *J. Hazard. Mater.*, 2019, **367**, 91.
72 Y. Li and D. Sen, *Chem. Biol.*, 1998, **5**, 1.
73 X. Yang, C. Fang, H. Mei, T. Chang, Z. Cao and D. Shangguan, *Chem.–Eur. J.*, 2011, **17**, 14475.
74 A. F. Voter, Y. Qiu, R. Tippana, S. Myong and J. L. Keck, *Nat. Commun.*, 2018, **9**, 4201.
75 D.-M. Kong, J. Xu and H.-X. Shen, *Anal. Chem.*, 2010, **82**, 6148.
76 L. Stefan, D. Duret, N. Spinelli, E. Defrancq and D. Monchaud, *Chem. Commun.*, 2013, **49**, 1500.